

# In Vivo Real Time Raman Spectroscopy Detection of Carbon Nanotube Kinetics in Lymph, Blood and Tissues

Alexandru S. Biris<sup>1,\*</sup>, Ekaterina I. Galanzha<sup>2</sup>, Zhongrui Li<sup>1</sup>, Meena Mahmood<sup>1</sup>, Yang Xu<sup>1</sup>, Enkeleida Dervishi<sup>1</sup>, and Vladimir P. Zharov<sup>2</sup>

<sup>1</sup>Nanotechnology Center, Applied Science Department, University of Arkansas at Little Rock, AR, 72204, asbiris@ualr.edu

<sup>2</sup> Philips Classic Laser Laboratories, University of Arkansas for Medical Sciences, Little Rock, AR, 72205

## ABSTRACT

The development of novel therapies using unique nanostructures for molecular targeting has become a major area of biological research. Here, we present the first report of the use of carbon nanotubes (CNTs) as high contrast agents for time-resolved Raman spectroscopy with ultra-fast spectral acquisition times to study their absorption and distribution kinetics in lymph, blood, and tissues in live animals. Our results suggest that the strong and specific CNTs Raman scattering properties provide means for noninvasive Raman flow cytometry to analyze the *in vivo* CNTs pharmacokinetics. Moreover, the biodistribution in lymph, blood and tissues were successfully analyzed using this technique with potential for blood and lymph analysis and to track, in real time, drugs in tissues.

**Keywords:** carbon nanotube, real time raman, *in vivo*

## 1 INTRODUCTION

Carbon nanotubes (CNTs) have demonstrated great potential in biology and medicine because of their unique well-controlled physical and chemical properties promising novel molecular diagnoses and therapies for cancer and infections [1]. CNTs interact relatively quickly and travel through biological tissue, crossing blood vessel, and even the blood-brain barrier [3-4]. CNTs pharmacokinetics and biodistribution in living organisms were previously obtained *ex-vivo* using radioactive labeling or near-infrared (NIR) fluorescence techniques [4-5]. One of the major challenges in biological applications of CNTs is their *in vivo* real-time detection and identification, including CNT dynamic tracking, especially in the circulation. To date, most CNT-related studies were performed *ex-vivo* in static conditions because of the relatively long signal

acquisition algorithms of most of the existing methods [3-5]. Recently we demonstrated the capability of *in vivo* photoacoustic (PA) flow cytometry with NIR lasers for real-time monitoring of circulating single nanoparticles and pathogens labeled with CNTs [6-7]. Nevertheless, fast spectral identification of CNTs is still a major challenge because of slow spectral scanning in most available NIR lasers. An attractive alternative is micro Raman spectroscopy [8], which may offer molecular specificity and excellent signal-to-noise ratio for detection and identification of CNTs spectra due to strong Raman scattering signals and vibrational spectra features [9-10]. However, the low sensitivity of existing Raman spectroscopy techniques has, so far, limited their application for the dynamic study of biological processes *in-vivo*. The goal of this work is to analyze the “dynamic” capability of advanced time-resolved Raman spectroscopy with high sensitivity and spectral resolution using CNTs as unique Raman contrast agents. To our best knowledge, this is the first study that shows the ability of micro-Raman spectroscopy *to monitor in vivo and in real time the biodistribution of CNTs* in lymphatics within real complex biological environments.

## 2 EXPERIMENTAL SECTION

The feasibility studies of *in vivo* RFC involved rats as animal models (White Fisher, F344) approved by the Institutional Animal Care and Use Committee. After standard anesthesia (ketamine/xylazine, 60/15 mg/kg), an animal was placed on the automated stage of the Olympus microscope with a customized heated module (37.7°C) that was optically connected to the Raman spectrometer. The ear blood vessels examined were located 50-80  $\mu\text{m}$  deep with 40-50  $\mu\text{m}$  diameters and blood velocities of 1–5 mm/sec. Immediately after exposure, the mesentery was

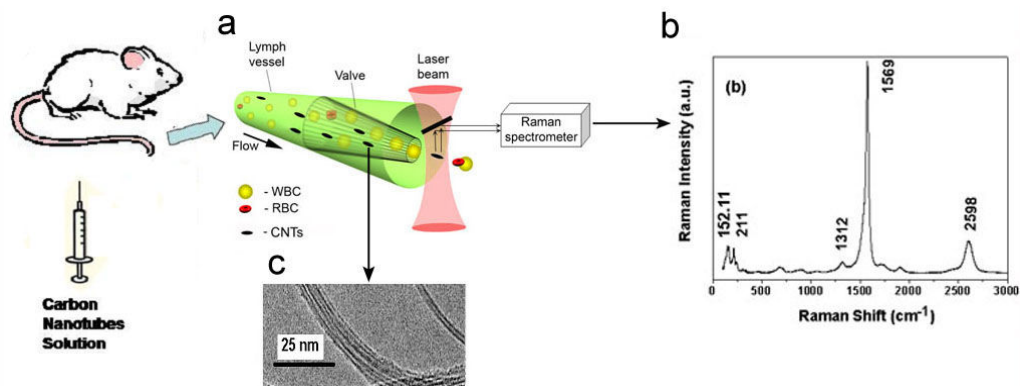
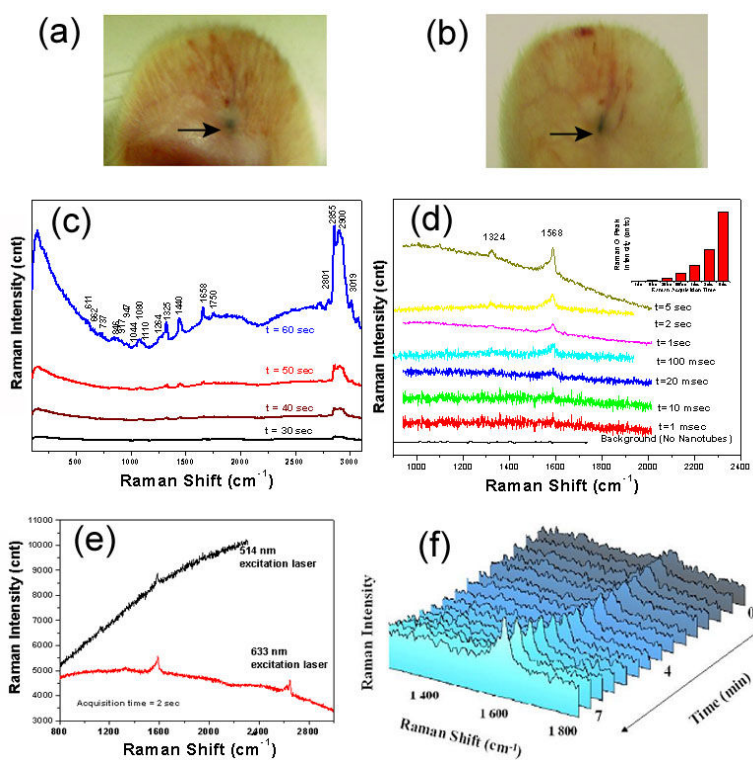


Figure. 1 Schematic of Raman flow cytometer for in vivo study (a), TEM image of the individual and bundled CNTs (b) and Raman scattering spectrum of CNT bundles in solution in vitro (c)



**Figure 2.** Optical images of local area of rat ear tissue at 10 (a) and 20 (b) minutes after CNT injections. (c) Raman spectra of rat ear tissue areas without CNTs as a function of the Raman spectrum acquisition time. (d) Raman spectra of rat ear tissue area with CNTs at 633 nm as a function of the acquisition time. (e). Raman spectra of rat ear tissue area with CNTs at two wavelength 514 nm, and 633 nm at the same power (10 mW) and acquisition time of 2 sec. (f) Raman spectra of rat ear tissue area on boundary of CNT distribution as function time at acquisition time of 2 sec. The time T=0 sec is the time of starting of spectra measuring (approximately 10 min after CNT injection).

placed on the heated stage and bathed in warm Ringer's solution (37°C, pH 7.4). Three sets of experiments were performed: (1) CNT solution was delivered with a 28 gage needle intravenously through the rat tail vein or (2) by local injection in the

ear regions and (3) by local administration in the rat mesentery. The laser beam was focused either on the interstitial ear tissue, blood or lymph ear microvessels, or in the mesentery vessels, depending upon the experiment performed.

### 3 RESULT AND DISCUSSION

The general schematic of the developed *in-vivo* Raman flow cytometer (RFC) is presented in Fig. 1a. The average length and diameter of individual CNTs obtained with TEM were 150-190 nm and 1.1-1.8 nm, respectively (Fig. 1b). The G band in the Raman spectra (Fig. 1c) has the highest intensity and therefore it was further used to evaluate the presence of CNTs in biological tissues. To estimate the *in vivo* maximal sensitivity of the technique in almost ideal static conditions, a small amount of CNT solution (10  $\mu$ l, concentration of 0.2 mg/ml) was locally injected under the skin of the rat ear in an area free of blood microvessels. Optical monitoring revealed that initially highly localized CNTs solution (Fig. 2a), shaped into an elongated zone after 20 minutes (Fig. 2b). The collection of the Raman spectrum of the CNT-free tissue with distinguished spectral features required relatively long acquisition times. Figure 2c shows representative Raman spectra (out of over 50) of the tissue collected *in-vivo* at 30, 40, 50, and 60 seconds acquisition times, along with the major peaks. It indicates the presence of fatty acids, DNA, RNA, and various proteins. Figure 2c indicates the even for relatively long acquisition times (over 60 seconds) the Raman spectra of the biological tissues did not show any peak at  $1568\text{ cm}^{-1}$ , which is specific to the G Raman band of CNTs (Fig. 1c). The slight peak at  $1568\text{ cm}^{-1}$  specific to CNTs (Fig. 1c) was already visible for as low as 1 ms acquisition times among background signals from the ear tissue (Fig. 2d). When the acquisition time was increased to 10 and then to 20 ms, the  $1568\text{ cm}^{-1}$  peak became better defined and increased in intensity. At 1 second acquisition time, besides the G band, the nanotubes' D band also became evident in the Raman spectra ( $1312\text{ cm}^{-1}$ ) (Fig. 2d). These data clearly indicate the difference in the Raman scattering of CNTs and biological tissue, especially at short acquisition time intervals ( $<10\text{ s}$ ) when there is a smooth background from tissue with no distinguished spectra feature (Fig. 2d, bottom). The analysis of the Raman spectra of tissue with CNTs collected at the two laser wavelengths revealed weaker Raman signal and higher scattering/fluorescence background at 514 nm compared to 633 nm (Fig. 2e). Spectral monitoring of tissue with the acquisition time of 2 s in an area close to the initial spot with high CNT concentration (see arrow in Fig. 1a) as a function of time and with the starting analysis time of 10 min after CNT injection, demonstrated a gradual increase of the  $1568\text{ cm}^{-1}$  peak intensity indicating continuous increased concentration of CNTs at the point of analysis due to bio-redistribution of CNTs.

Taking into account a previous lymphatic study [34], the obtained kinetic data strongly suggested that CNTs, after their migration in tissue, were uptaken by the neighboring lymph vessels followed by their further propagation in lymphatics. Indeed, CNTs pure tissue diffusion provides usually a relatively homogenous distribution around the injected area while both the optical image and Raman spectra indicated a significant increase of CNT concentration in one dominant direction likely associated with lymph microvessels.

To further verify this finding of CNT uptake by lymphatics, a mesentery model with clearly distinguished individual lymph vessels was studied with RFC. The CNT solution (100  $\mu$ l, concentration of 0.05 mg/ml) was topically administered on the mesentery surface, followed by Raman detection of the CNTs in the 150-200  $\mu$ m diameter lymph vessels. The laser beam was focused onto the area after the lymph valve, which acts as a natural nozzle concentrating flowing CNTs near vessel axis [11].

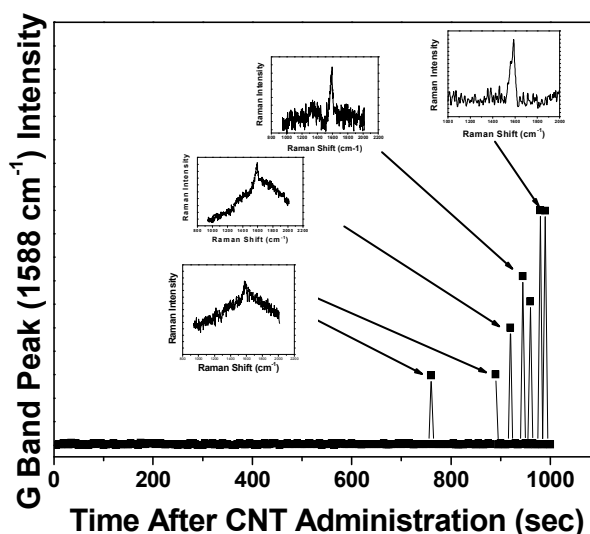


Figure 3. The intensity of the  $1568\text{ cm}^{-1}$  peak (G band) from a lymph vessel as a function of time after CNTs administration (b). The time  $T=0\text{ sec}$  is considered the time of CNTs delivery in mesentery.

Raman detection was performed by collecting and analyzing the  $1568\text{ cm}^{-1}$  peak intensity (G band for CNTs), which is in direct relationship with the number of CNTs present in the focal volume of the excitation He-Ne laser beam. Taking into consideration the laser scattering phenomena in tissue this volume was estimated to be of approximately  $30\text{ }\mu\text{m}^3$ . As shown by Figure 3b, the time required for the peak at  $1568\text{ cm}^{-1}$  to become present in the

Raman spectra of the lymph vessels was approximately 12 min. Raman data indicated that the intensity of the G band increased with measurement time, which indicates a continuous increase of CNT concentration in the lymph vessels due to the CNTs uptaking from the surrounding interstitial tissue. To avoid background Raman signals due to the CNTs possibly present on the mesentery surface, the surface of the area exposed to the laser radiation was continuously washed with warm Ringer's solution. This procedure did not influence the Raman signal levels of the lymphatic system, suggesting the presence of CNTs mainly inside the lymph vessels.

Therefore, the CNTs were found to present a high mobility and ability to travel through the interstitial tissue, to enter into the lymph system, and to propagate through the lymphatics. The distribution rate of CNTs in lymph vessels depends on the activity of these vessels, which in rat mesentery varies between a complete absence of lymph flow, low flow velocity in the range of 0.05-0.2 mm/s (as observed for the vessels that were analyzed in this study) and relatively high flow velocity up to 0.5 -1 mm/s, and even more in limited vessels [11].

Preliminary experiments with intravenous injection of CNTs in the tail vein indicated the appearance of rare low level fluctuated Raman signals in the 50-70  $\mu\text{m}$  ear blood microvessels during the first 1 to 5 minutes after injection, when likely a relatively large numbers of CNTs became present in the blood system and therefore also in the measurement volume. No Raman signals of the 1568  $\text{cm}^{-1}$  peak were observed 5 minutes after injection, probably because of the fast CNT clearance rate [7] and the short laser exposure time of the fast moving individual CNTs through the detected volume. Indeed, the travel time of individual CNTs through the width of the laser beam (few  $\mu\text{m}$ ) at 3-5 mm/s blood flow velocity [11] was estimated to be around 1 ms, which as shown in Fig. 2d, is close to the threshold sensitivity of the Raman instrument used for these studies. Nevertheless, additional improvement of the signal acquisition algorithm by using optimized spectral range could approach the sensitivity threshold of as few as one individual CNT present in the detected volume at 1 ms time acquisition.

#### 4 CONCLUSION

In summary, the original experimental data presented in this report indicates that Raman spectroscopy previously used to study biological systems in stationary conditions was successfully extended to dynamic studies of biological processes due to the unique properties of CNTs as high contrast Raman

agents and advances in fast Raman signal acquisition. As a result, it was shown for the first time the high ability of CNTs to distribute in tissue and accumulate and further travel through the lymphatic systems. *In vivo* Raman flow cytometry technique can be considered as a new tool in biological research, with advanced capabilities to detect individual CNTs with average velocities of 0.1 mm/s typical to lymphatics and at least approximately 10-50 CNTs present in the detected volume moving at velocities of up to 5 mm/sec that is typical for blood microcirculation. These findings open the opportunity for real-time Raman detection and identification of circulating cancer cells, bacteria, or other objects labeled with bioconjugated CNTs before their dissemination induces metastasis and sepsis. The ability of CNTs to provide strong both Raman, photothermal, and photoacoustic signals, allows the integration of all these methods in one technical flow cytometry platform which could become more universal and applicable to objects with various absorption and Raman scattering properties.

#### REFERENCES

1. N.W.S. Kam, M. O'Connell, J.A. Wisdom, H. Dai, *Proc. Natl. Acad. Sci. USA*, 102,11600-11605, 2005.
2. M. Ferrari, *Nature Reviews*, 5, 161-171, 2005.
3. N. L. Mills, N. A. Simon, D. Robinson, A. Anand, J. Davies, D. Patel, J. M. de la Fuente, F. R. Cassee, N. A. Boon, W. MacNee, A. M. Millar, K. Donaldson and D. E. Newby, *American Journal of Respiratory and Critical Care Medicine* 173, 426-431, 2006.
4. J. Guo, X. Zhang, W. Li, *Nuclear Medicine and Biology*, 34, 579-583, 2007.
5. P. Cherukuri, C. J. Gannon, T. K. Leeuw, H. K. Schmidt, R. E. Smalley, S. A. Curley, and R. B. Weisman, *Proc. Natl. Acad. Sci. USA* 103, 18882-18886, 2006.
6. V. P. Zharov, E. I. Galanzha, E. V. Shashkov, V. V. Tuchin, *Optics Lett.* 31,3623-3625, 2006.
7. V. P. Zharov, E. I. Galanzha, E. V. Shashkov, J. W. Kim, N. G. Khlebtsov, V. V. Tuchin, *J Biomed Opt*, 12, 0551503, 2007.
8. J. T. Motz et al., *J Biomed Optics* 10, 031113, 2005.
9. M. S. Dresselhaus, G. Dresselhaus, A. Jorio, A. G. Souza Filho, R. Saito, *Carbon* 40, 2043, 2002.
10. A. Jorio, M. A. Pimenta, A. G. Souza Filho, R. Saito, G. Dresselhaus, M. S. Dresselhaus, *New J. Phys.* 5, 13, 2003.
11. E. I. Galanzha, V. V. Tuchin, and V. P. Zharov, *World J Gastroenterol* 13,192-218, 2007.